Solution Approach to Automatic Generation Control Problem Using Hybridized Gravitational Search Algorithm Optimized PID and FOPID Controllers

Preeti DAHIYA[1], Veena SHARMA[2], Ram NARESH[3]
[1,2,3]*National Institute of Technology, Hamirpur, Himachal Pradesh, 177005, India*
[1]*preetieed@nith.ac.in,* [2]*veena@nith.ac.in,* [3]*rnaresh@nith.ac.in*

***Abstract*—This paper presents the application of hybrid opposition based disruption operator in gravitational search algorithm (DOGSA) to solve automatic generation control (AGC) problem of four area hydro-thermal-gas interconnected power system. The proposed DOGSA approach combines the advantages of opposition based learning which enhances the speed of convergence and disruption operator which has the ability to further explore and exploit the search space of standard gravitational search algorithm (GSA). The addition of these two concepts to GSA increases its flexibility for solving the complex optimization problems. This paper addresses the design and performance analysis of DOGSA based proportional integral derivative (PID) and fractional order proportional integral derivative (FOPID) controllers for automatic generation control problem. The proposed approaches are demonstrated by comparing the results with the standard GSA, opposition learning based GSA (OGSA) and disruption based GSA (DGSA). The sensitivity analysis is also carried out to study the robustness of DOGSA tuned controllers in order to accommodate variations in operating load conditions, tie-line synchronizing coefficient, time constants of governor and turbine. Further, the approaches are extended to a more realistic power system model by considering the physical constraints such as thermal turbine generation rate constraint, speed governor dead band and time delay.**

***Index Terms*—automatic generation control, disruption operator, fractional calculus, gravitational search algorithm, opposition based learning.**

I. INTRODUCTION

In an interconnected power system, the purpose of automatic generation control (AGC) is to achieve better frequency regulation and maintain the tie-line power flow at scheduled level irrespective of load changes in an area. In order to implement AGC, the system parameters such as frequency, tie line power flow and individual generator outputs are monitored continuously. Based upon the monitored information and reference values of frequency and tie line power, area control errors (ACE) which are a linear combination of tie line power mismatch and frequency deviations are computed. The area control errors are sensed by the designed controllers, which generate control signals for establishing new generator set points whenever load occurs in the system. The minimization of ACE results in reduction in both frequency and tie-line power errors [1]. The researchers in this field are trying to understand and implement several strategies for AGC of power systems. The authors in [2-4] critically reviewed various control schemes such as classical, optimal [5], sub-optimal [6], adaptive, soft computing [7-9] etc. for conventional and distributed generation power systems. These approaches are not simple and need thorough knowledge and familiarity among users to implement these methods. The proportional integral derivative (PID) controller is structurally simple and reliable for implementation. The fractional order proportional integral derivative (FOPID) controller has two additional parameters of non-integer order of integration and differentiation and this feature of FOPID provides more flexibility and accuracy to the controller design [10]. The major concern of these controllers is the optimal tuning of their several parameters. Literature survey shows that in recent past, meta-heuristic optimization techniques have been used to optimize the controller parameters for AGC system such as genetic algorithm (GA), particle swarm optimization (PSO) [11-13], bacterial foraging optimization (BFO) [14], differential evolution (DE) [15], imperialist competitive algorithm (ICA) [16], firefly algorithm (FA) [17] etc. These types of heuristic optimization approaches are frequently being used because they easily handle the inherent non-linearities such as generation rate constraint (GRC), governor deadband etc. present in the AGC system. In the literature, various authors have tried to prove the superiority of one technique over the other in terms of performance parameters like premature convergence, reduction in search capability, robustness and precision etc. Therefore, the researchers are trying to develop and implement more and more efficient algorithms to deal with the complex AGC problems. The present work is an attempt towards tuning of PID and FOPID controller parameters for optimum performance using gravitational search algorithm and its variants. The gravitational search algorithm (GSA) introduced in [18] is based on Newtonian gravity and it has been reported in the literature that GSA is efficient in terms of computation time and gives more accuracy while solving optimal problems [19-20]. The convergence speed and solution quality are affected by population initialization in all the heuristic algorithms. The quality of population initialization is enhanced by using the opposition based learning concept [21-22]. A balance between exploration and exploitation ability for optimal search is maintained by employing a disruption operator introduced in [23]. The investigation of the search space for new and better solutions

Digital Object Identifier 10.4316/AECE.2015.02004

refers to exploration and exploitation is the capability of algorithm to search a better solution near a good one. Having known all this, an attempt has been made in this paper to tune the PID and FOPID controller parameters using a novel disruption based opposition learned gravitational search algorithm. The objectives of the present work are as follows:

i. to tune the PID and FOPID controller parameters of four area interconnected power system using hybridized disruption based opposition learned gravitational search algorithm.
ii. to compare the results of DOGSA tuned controllers with GSA, OGSA and DGSA to investigate the superiority of the optimization algorithm.
iii. to demonstrate the robustness of DOGSA tuned PID and FOPID controllers to wide variations in the system parameters, sensitivity analysis is performed.
iv. to study the effect of the physical constraints such as thermal turbine generation rate constraint, speed governor dead band and time delay caused during signal processing on the system performance.

The description of modeling of four area hydro-thermal-gas interconnected power system is presented in Section II. The mathematical model of PID and FOPID controllers are discussed in Section III. Section IV presents the optimization techniques used for tuning the gain parameters of the controllers. The simulation results of considered power system with PID and FOPID controllers optimized by GSA and its variants are presented in Section V. The next subsection gives the sensitivity analysis followed by the effect of generation rate constraint, time delay and governor deadband. The conclusion based on the simulation results is discussed in Section VI.

II. System Modeling

The four area power system hydro-thermal-gas plant connected by tie-line is shown in Fig. 1. The fourth area is considered to have infinite kinetic energy i.e. free energy source which implies that the frequency deviations did not matter in this area [5, 24]. The inputs to each control area are the controller outputs (u_k), load disturbances (d_k), and tie-line power error ΔP_{tiek} for an area k. The outputs are the generator frequency deviations (Δf_k) and area control error (ACE_k) given as:

$$ACE_k = \sum_{j=1}^{n} \Delta P_{kj} + B_k \Delta f_k \tag{1}$$

ΔP_{kj} is the tie line power flow from area k to area j and B_k is the bias factor. Each control area comprises of speed governor, turbine and load whose transfer functions are given in Fig. 1. The symbols and parameters of the considered interconnected power system are given in Appendix A and Appendix B.

III. Mathematical Model of PID and FOPID Controller

The fractional order (FO) theory deals with the differential equations of non-integer order. The fractional calculus is the generalization of integer order (IO) calculus. The FOPID controller has the notion given by $PI^{\lambda}D^{\mu}$ where λ and μ are non-integer orders of integrator and differentiator respectively. The controlled action of $PI^{\lambda}D^{\mu}$ controller for considered interconnected power system can be expressed as:

$$u(t) = K_p e(t) + K_i \left(\frac{d}{dt}\right)^{-\lambda} e(t) + K_d \left(\frac{d}{dt}\right)^{\mu} e(t) \tag{2}$$

where $e(t)$ is the input area control error signal, $u(t)$ is controller output, K_p, K_i and K_d are proportional, integral and derivative gains respectively. The additional tuning knobs λ and μ in FOPID controller offers better flexibility and system dynamics than the integral order proportional integral derivative (IOPID) controller [10]. The laplace transfer function of FOPID controller of generator n is given as:

$$G_n(s) = K_p + \frac{K_i}{s^{\lambda}} + K_d s^{\mu};\ \text{n=1,2,3,4,5} \tag{3}$$

When the value of λ and μ are equal to unity, it gives the transfer function of IOPID controller. The fractional derivative or integral s^{ρ}, where ρ is a non-integer number can be approximated by Oustaloup recursive filter in pre-specified frequency range $[\omega_l, \omega_u]$, where ω_l and ω_u is the lower and upper frequency limits of approximate transfer function [10] expressed as:

$$s^{\rho} \approx A \frac{ps^2 + qs\omega_u}{p(1-\rho)s^2 + qs\omega_u + p\rho} \prod_{i=-N_f}^{N_f} \frac{s+\omega_i'}{s+\omega_i} \tag{4}$$

where, constant gain, frequency of zeros and poles are determined by:

$$A = \left(\frac{p\omega_l}{q}\right)^{\rho} \prod_{i=-N_f}^{N_f} \frac{\omega_i}{\omega_i'};\ \omega_i' = \left(\frac{p\omega_l}{q}\right)^{(\rho-2i)/(2N_f+1)};$$
$$\omega_i = \left(\frac{q\omega_u}{p}\right)^{(\rho+2i)/(2N_f+1)} \tag{5}$$

where N_f is number of zeros and poles, p and q are small constant gains.

IV. Controller Tuning using Heuristic Optimization Techniques

This section gives a brief overview of basic GSA, opposition learning and disruption operator. Then, the pseudo code for hybridized DOGSA approach to obtain optimal parameter values is given which gives the advantages of fast convergence and better exploration & exploitation of the search space. The optimization of the controller gains corresponds to the minimum deviations in frequency and tie-line power. The overall fitness function, integral time absolute error (ITAE) for the optimization problem in present work is:

$$F = \int_0^T t \times \sum_{k=1}^{3} \left(|\Delta f_k| + |\Delta P_{tiek}|\right) dt \tag{6}$$

where Δf_k and ΔP_{tiek} are deviations in frequency and tie-line power in area k for k =1, 2, 3 and T is the time interval over which fitness function is evaluated. The fitness function penalizes the deviations in frequency and tie-line power that persist for long periods of time. The figure of demerit (FOD) is also calculated whose minimum value indicates the minimization of the overshoot (OS) and steady state value (SV) of deviations in frequency and tie-line power.

$$FOD = \sum_{k=1}^{3} (OS(\Delta f_k))^2 + (SV(\Delta f_k))^2 + (OS(\Delta P_{tiek}))^2 + (SV(\Delta P_{tiek}))^2 \tag{7}$$

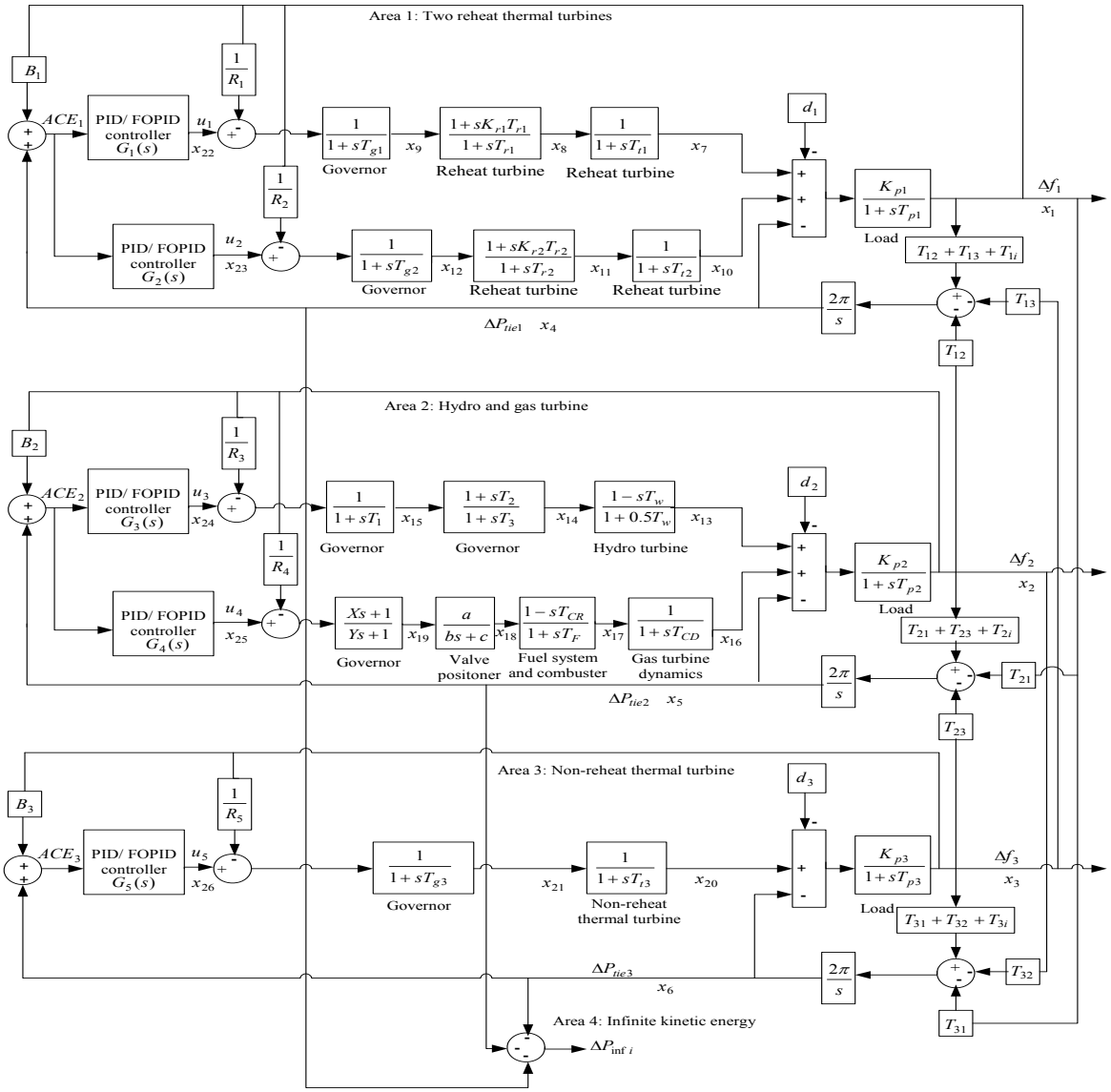

Figure 1. Transfer function block diagram

The state space model of the system is developed using the state variables vector:

$$X = [\Delta f_1\ \Delta f_2\ \Delta f_3\ \Delta P_{tie1}\ \Delta P_{tie2}\ \Delta P_{tie3}\ \Delta P_{t1}\ \Delta P_{r1}\ \Delta P_{g1}\ \Delta P_{t2}\ \Delta P_{r2}\ \Delta P_{g2}\ \Delta P_{tw}\ \Delta P_{G2}\ \Delta P_{G1}\ \Delta P_{TD}\ \Delta P_{FC}\ \Delta P_{vp}\ \Delta P_{sg}\ \Delta P_{t3}\ \Delta P_{g3}\ ACE_1G_1(s)\ ACE_1G_2(s)\ ACE_2G_3(s)\ ACE_2G_4(s)\ ACE_3G_5(s)]$$

A. Gravitational Search Algorithm

GSA is a heuristic optimization algorithm based on Newton's law of gravity and motion [18]. For tuning of PID controller, the masses correspond to the controller gains and the performance is the fitness function given by equation (6). To describe the GSA, consider a system with N_p controller gains in which the position of the i^{th} gain is defined by:

$$U_i = (u_i^1, ..., u_i^d, ..., u_i^n) \text{ for } i = 1,2, \ldots\ldots, N_p \quad (8)$$

where u_i^d denotes the position of the i^{th} gain in the d^{th} dimension and n is the dimension of the search space. The positions of gains in the search space correspond to the optimal solution. The acceleration of the gain *i* at time *t*, and in direction d^{th} according to law of motion ($a_i^d(t)$), is:

$$a_i^d(t) = \frac{f_i^d}{W_i(t)};\ f_i^d = \sum_{j=1 j\neq i}^{N_p} rand_j \times G(t) \times \frac{W_i(t) \times W_a(t)}{\left(R_{ij}(t) + \varepsilon\right)} \times (u_j^d(t) - u_i^d(t))$$

$$G(t) = G_0 e^{-\alpha \times t / iter_{\max}} \quad (9)$$

where f_i^d is force acting on gain *i*, W_i is the inertial mass of i^{th} gain, W_a is the gravitational active mass, *G(t)* is gravitational constant at time *t*, G_0 is initial gravitational constant, ε is small constant, α is small decaying constant, $rand_j$ is a random number in the interval [0, 1] and $R_{ij}(t)$ is the euclidian distance between two gains *i* and *j*. The fitness evaluation gives the inertial mass. An agent (controller gain) is more efficient if it has more mass. This means that better gains have higher attractions and move more slowly. The inertial masses are updated by the following equation:

$$W_i(t) = \frac{F_i(t) - w(t)}{(b(t) - w(t)) \times \sum_{j=1}^{N} m_j(t)} \quad (10)$$

where $F_i(t)$ denotes the fitness value of the gain *i* at time *t*, and, *w(t)* and *b(t)* are defined as follows for a minimization problem:

$$b(t) = \min_{j \in \{1,2..N\}} F_j(t) \quad (11)$$

$$w(t) = \max_{j\in\{1,2..N\}} F_j(t) \tag{12}$$

The updation of position and velocity of controller gains in search space is done as:

$$u_i^d(t+1) = u_i^d(t) + v_i^d(t+1) \tag{13}$$

$$v_i^d(t+1) = rand_i \times v_i^d(t) + a_i^d(t) \tag{14}$$

where $rand_i$ is a uniform random variable in the interval [0, 1].

B. Opposition based Learning

The evolutionary optimization algorithms are population based techniques which are aimed at finding the optimal solutions to the problem. The random presumptions are made at the beginning about the solution. The computational time for searching optimal solution can be reduced by concurrently checking the opposite solution [21]. This helps in choosing the better solution as an initial solution and hence, increases the potential to accelerate convergence of the algorithm. Let $U = (u_1, u_2, ..., u_d)$ be a point in d-dimensional space, where $u_1, u_2, ..., u_d \in R$ and $u_i \in [a_i, b_i] \forall_i \in \{1, 2, ..., d\}$. The opposite point is defined by [18]:

$$\breve{u}_i = a_i + b_i - u_i \tag{15}$$

The fitness function given by equation (6) is used to calculate the individual fitness at both u_i and $\breve{u}_i$. If $f(\breve{u}) \geq f(u)$, then point $\breve{u}$ can be replaced with u else continue with $\breve{u}$. The GSA based on this opposition based population initialization is called as OGSA.

C. Disruption Operator

The exploration and exploitation abilities of GSA are enhanced using novel operator called disruption which is originated from astrophysics [23]. For the simulation of the disruption process, it is assumed that the best solution (agent with heaviest mass) is the star of the system, and the other solutions can potentially disrupt and scatter in space under the gravity force of the star. The solutions that satisfy the condition given by equation (16) below become disrupted so as to prevent divergence in solutions [23].

$$\frac{R_{i,j}}{R_{i,best}} < K \;;\; R_{i,best} = \| u_i(t), u_{best}(t) \|_2 \;;\; K = \tau\left(1 - \frac{t}{iter_{\max}}\right) \tag{16}$$

where $R_{i,j}$ is euclidian distance between masses i and j, $R_{i,best}$ is euclidian distance between mass i and the best solution, K is threshold value, τ is small constant, t is current iteration and $iter_{max}$ is total number of iterations. The position of every mass (solution) that satisfies equation (16) will change, according to the following equation:

$$U_i(new) = U_i(old).D \tag{17}$$

$$\text{where } D = \begin{cases} R_{i,j} \times c(-0.5, 0.5) & if\ R_{i,best} \geq 1 \\ (1 + \beta \times c(-0.5, 0.5)) & otherwise \end{cases} \tag{18}$$

In equation (18), *c(−0.5, 0.5)* returns a uniformly distributed pseudo random number in the interval [−0.5, 0.5]. U_i is the position of mass i that should be disrupted and β is a small number. The GSA incorporating the disruption operator is called DGSA.

D. Hybridized Disruption based Opposition Learned GSA (DOGSA)

A more recent hybridized DOGSA technique is introduced to incorporate the advantages of both opposition based learning to increase the convergence rate of optimization algorithm and disruption operator to have a good balance between exploration and exploitation to achieve both efficient global and local searches. The pseudo code of DOGSA optimization technique is given below:

Step 1: Initialize population P_0 with controller gains
Step 2: Initialize population OP_0 with opposite presumptions
for (i=0;i<N_p;i++) % N_p is the size of population
  for(j=0;j<d;j++) % *d* is the dimension of problem
  $OP_{i,j} = a_j + b_j - P_{0i,j}$
end
Step 3: Evaluate the fitness function using equation (6)
Step 4: Rank the fitness function based on their evaluated value. Select N_p individuals from the set of $\{P_0, OP_0\}$ based on the minimum fitness function as initial population P
Step 5: Calculate $W_i(t)$, $b(t)$ and $w(t)$ using equation (10), equation (11) and equation (12)
Step 6: Calculate forces in all directions according to equation (9)
Step 7: Update positions and velocities of all gains using equation (13) and equation (14)
Step 8: Disrupt the positions u_i using equation (17) and equation (18)
Step 9: Repeat steps 3-7 until stopping criterion is met

V. Results and Discussions

This section presents simulation results of four area AGC interconnected power system using stochastic heuristic approach GSA and its variants such as OGSA, DGSA and DOGSA tuned PID and FOPID controllers. For each of the algorithms, integral time absolute error fitness function has been used to find the optimal gains of controllers. In this paper, the minimum limit of each of K_p, K_i, K_d is -10 and the maximum limit is 10 and for λ and μ, minimum and maximum values are chosen as 0 and 2. Each generating area has its individual controller which increases the flexibility of the system. The controller parameters chosen for the application of optimization algorithms are: population size N_p=30; maximum iteration $iter_{max}$=1000, G_0=100, α=20, τ=100 and β=10^{-16}. The frequency range for Oustalop approximation is taken to be [0.01 100] and N_f =5. The settling time and steady state values are calculated considering an error band of 1%.

A. Comparison of GSA, OGSA, DGSA and DOGSA Tuned PID Controller

The optimization techniques GSA, OGSA, DGSA and DOGSA are implemented to tune the PID controller gains for four area AGC system when a step load perturbation of 0.1 p.u MW is considered in all the areas. The convergence profiles of all the optimization algorithms are shown in Fig. 2. The general trend observed from these characteristics is that all the presented algorithms quickly bring down the fitness function during initial iterative process. As expected GSA, OGSA, DGSA and DOGSA saturate to fitness values

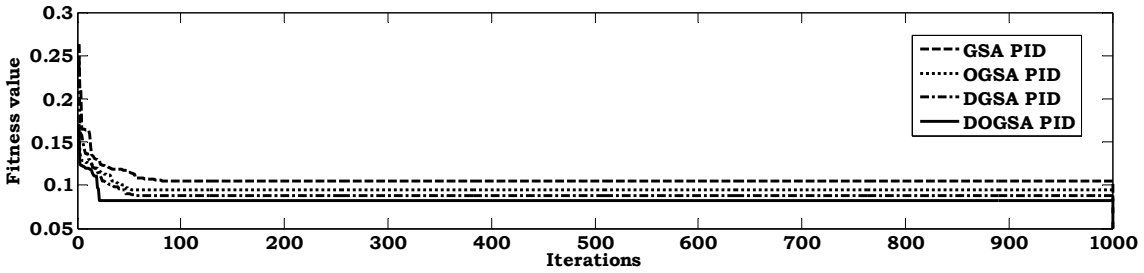

Figure 2. Comparative convergence profiles of GSA, OGSA, DGSA and DOGSA optimized PID controller

which are 0.1046, 0.0945, 0.0874 and 0.0823 respectively. The best performance of DOGSA giving least fitness value is attributed to its better exploration and exploitation capabilities. The eigen values depicting the relative stability of the system, damping ratio, settling time and peak overshoot of frequency and tie-line power deviations of the system, ITAE fitness function and figure of demerit (FOD) values are given in Table I for PID controller. The dynamic responses are shown for area 1 only.

Although, all the eigen values of system without controller lies on left side of s-plane, yet the tie-line power deviations does not reach their steady state. The optimized PID diminishes the perturbation in frequency and scheduled tie line power to their steady state values. Examining the performance criterion values from Table I and dynamic responses from Fig. 3 and Fig. 4, it is observed that the DOGSA tuned PID controlled system has minimum integral time absolute error, damping ratio, settling time and peak overshoot as compared to its other variants.

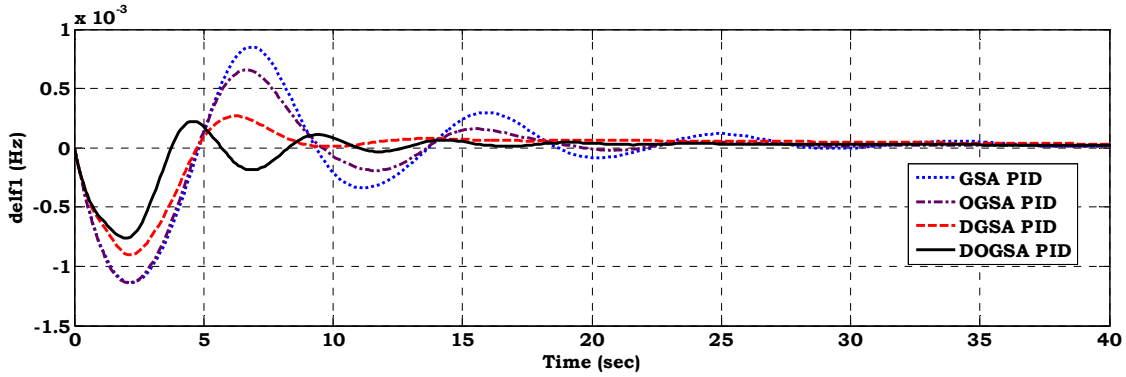

Figure 3. Frequency deviation in area 1 with optimized PID controller

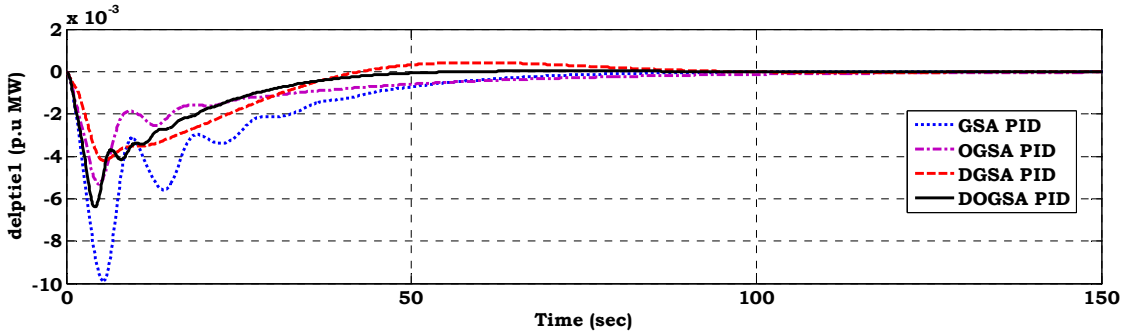

Figure 4. Tie-line power deviation in area 1 with optimized PID controller

The figure of demerit is also minimum for DOGSA optimized PID controlled system which signifies the minimum settling time and peak overshoot of deviations in frequency and tie-line power. The optimized gains of these controllers are given in Table II.

TABLE I. COMPARISON OF EIGEN VALUES, DAMPING RATIO, SETTLING TIME, PEAK OVERSHOOT, FITNESS FUNCTION AND FIGURE OF DEMERIT VALUES FOR OPTIMIZED PID CONTROLLED SYSTEM

Parameters	Without Controller	GSA	OGSA	DGSA	DOGSA
Eigen Values	-12.5034	-12.5065	-12.5064	-12.5029	-12.5066
	-12.5104	-12.5015	-12.5003	-12.5098	-12.4997
	-4.7057 ± 0.2425i	-4.9778	-4.7027 ± 0.2196i	-4.7070 ± 0.2482i	-4.6900 ± 0.1068i
	-0.0446 ± 1.0687i	-4.3221	-2.7270	-2.5528 ± 0.3420i	-2.6860
	-0.0539 ± 1.0646i	0.0765 ± 1.2800i	-2.6692	0.0435 ± 1.1325i	-2.5723 ±0.1984i
	-0.0561 ± 0.5354i	0.0450 ± 1.1070i	-2.3718	-0.0301 ± 1.0814i	-0.0944 ± 1.3170i
	-0.9574	-2.6734	0.0836 ± 1.3133i	-2.4800	-0.0373 ± 1.1395i

	-2.6595 -2.3177 -2.4522 -1.9675 -0.0205 -0.0990 -0.1002 -2.5000 -2.0000 -0.1000	-2.5357 ± 0.0779i -0.0087 ± 0.6130i -1.1277 -2.0461 -2.0000 -2.5000 -0.0488 -0.0198 ±0.0208i -0.0158 -0.1044 -0.0989 -0.1000 -0.0000 -0.0000	-0.0014 ± 1.1092i -1.9685 -2.0000 -0.9423 -0.0283±0.5977i -2.5000 -0.1388 -0.1084 -0.0308 ± 0.0254i -0.0063 -0.0104 -0.1000 -0.0000 -0.0000	-1.9630 -2.0000 -0.9282 -0.0285 ±0.5611i -0.0285 - 0.5611i -2.5000 -0.0943 ±0.0408i -0.0943 - 0.0408i -0.1115 -0.0254 ± 0.0313i -0.0234 -0.1000 -0.0000 -0.0000	-1.9863 -2.0000 -1.0052 -0.0173±0.6194i -2.5000 -0.1488 -0.0651 ±0.0306i -0.0328 -0.0089 -0.0080 -0.1000 -0.0000 ± 0.0000i
Damping Ratio	0.0417	0.0141	0.0012	0.0279	0.0236
Settling Time (sec)					
Δf_1	73.10	34.37	25.03	25.01	21.33
Δf_2	78.80	37.67	26.42	29.48	25.24
Δf_3	68.20	38.09	28.04	24.86	21.94
ΔP_{tie1}	71.50	101.80	144.37	96.57	63.09
ΔP_{tie2}	88.40	211.10	145.10	144.50	160.90
ΔP_{tie3}	66.30	294.70	243.10	248.80	174.90
Peak overshoot					
Δf_1	0.001175	0.0008501	0.0006584	0.0002684	0.0002238
Δf_2	0.001148	0.0008772	0.0006091	0.0003999	0.0003496
Δf_3	0.001190	0.0008293	0.0006185	0.0003469	0.0002345
ΔP_{tie1}	-0.01704	-0.009886	-0.005301	-0.004194	-0.006406
ΔP_{tie2}	-0.01680	-0.013410	-0.012800	-0.012600	-0.009537
ΔP_{tie3}	-0.01678	-0.008562	-0.007700	-0.001470	-0.005298
Steady state values					
Δf_1	-0.0000311	0.0000561	0.0000470	0.0000555	0.0000272
Δf_2	-0.0000212	0.0000017	0.0000120	0.0000117	0.0000115
Δf_3	0.0000408	0.0000135	0.0000118	0.0000115	0.0000113
ΔP_{tie1}	-0.0098410	-0.0000185	-0.0000336	-0.00000075	0.0000167
ΔP_{tie2}	-0.0100060	0.0000499	0.0000729	-0.0000268	-0.0000916
ΔP_{tie3}	-0.0101300	-0.0000514	-0.0000480	-0.0000725	-0.0000725
ITAE fitness value	-	0.1046	0.0945	0.0874	0.0823
FOD	-	0.000353	0.000252	0.000179	0.000160

B. Comparison of GSA, OGSA, DGSA and DOGSA Tuned FOPID Controller

The convergence profiles of fitness values of GSA, OGSA, DGSA and DOGSA tuned FOPID controlled interconnected system is shown in Fig. 5. The fitness values are saturated to 1.6736, 1.4742, 1.2238 and 1.1522 for GSA, OGSA, DGSA and DOGSA respectively. The exploration and exploitation capabilities of DOGSA enable it to achieve the minimum fitness value in 55 iterations only. The eigen values, damping ratio, settling time, peak overshoot, fitness function and figure of demerit values for optimal FOPID controlled system are given in Table III.

TABLE II. OPTIMIZED PARAMETERS OF PID AND FOPID CONTROLLERS

Parameter	**PID**					**FOPID**				
	Initial values (Before optimization)	**GSA**	**OGSA**	**DGSA**	**DOGSA**	**Initial values (Before optimization)**	**GSA**	**OGSA**	**DGSA**	**DOGSA**
K_{p1}	-3.5010	4.1205	3.0257	1.8027	-4.8601	0.8042	0.5254	0.5729	0.3524	1.6662
K_{i1}	2.0308	1.5353	-2.8987	3.3507	4.7489	0.0314	0.0447	0.0312	0.0511	0.0580
K_{d1}	-4.5438	2.2709	3.6301	4.4628	4.7406	4.6400	1.0844	6.0844	5.8209	9.3220
λ_1	-	-	-	-	-	1.9627	1.5316	1.3120	1.6370	1.6721
μ_1	-	-	-	-	-	0.7233	0.7623	0.7115	0.7716	0.9127
K_{p2}	-4.3785	-1.4271	-3.7641	-4.9564	-3.2687	0.6804	0.5680	0.7498	4.7833	2.8702
K_{i2}	-3.5042	4.2183	2.2584	3.0313	2.8394	0.0079	0.0874	0.0128	0.0662	0.0960
K_{d2}	-1.2064	-0.4860	1.3285	-0.2105	-4.8444	11.6187	2.6566	1.4086	6.3415	1.8104
λ_2	-	-	-	-	-	1.2549	1.2222	1.0619	1.6074	1.4603
μ_2	-	-	-	-	-	0.7654	0.7192	0.7159	0.7259	0.7015
K_{p3}	-2.8794	0.2738	-4.0111	2.7211	-2.5686	0.9972	0.0965	0.0166	0.0244	0.0236
K_{i3}	-3.9710	-3.4289	-4.8503	2.9749	-1.7065	0.0295	0.0299	0.0234	0.0255	0.0229
K_{d3}	4.8681	0.6248	4.7562	-4.5950	0.0836	1.5793	0.7243	4.0751	0.9766	5.7880
λ_3	-	-	-	-	-	0.1356	1.4201	1.4441	1.5568	1.6530
μ_3	-	-	-	-	-	0.7337	0.7581	0.7706	0.7363	0.7728
K_{p4}	4.1579	-2.5089	0.0513	-1.4624	0.5753	0.3602	0.0673	0.0116	0.0924	0.0001
K_{i4}	3.0077	0.8999	2.2554	-2.3394	-1.2381	0.0040	0.0247	0.0345	0.0291	0.0330
K_{d4}	-4.5800	-3.4513	-0.4474	4.3253	3.6706	4.5944	0.0136	0.0256	0.0216	0.0195
λ_4	-	-	-	-	-	1.7005	1.5766	1.6032	1.3037	1.4672
μ_4	-	-	-	-	-	0.7896	0.7499	0.7805	0.7999	0.7260
K_{p5}	1.5249	-2.0176	-0.1260	-2.7869	-1.2885	0.2486	1.6304	0.8311	0.2246	1.0928

K_{i5}	3.0571	-1.2252	0.4366	-1.4046	-1.4560	0.0108	0.0633	0.0215	0.0918	0.0993
K_{d5}	1.8484	-1.0604	-3.7738	-0.3234	2.0932	4.9881	0.6657	0.9569	1.0191	8.2022
λ_5	-	-	-	-	-	1.7004	1.7751	1.5437	1.4924	1.3127
μ_5	-	-	-	-	-	0.7086	0.7371	0.7869	0.7109	0.7545

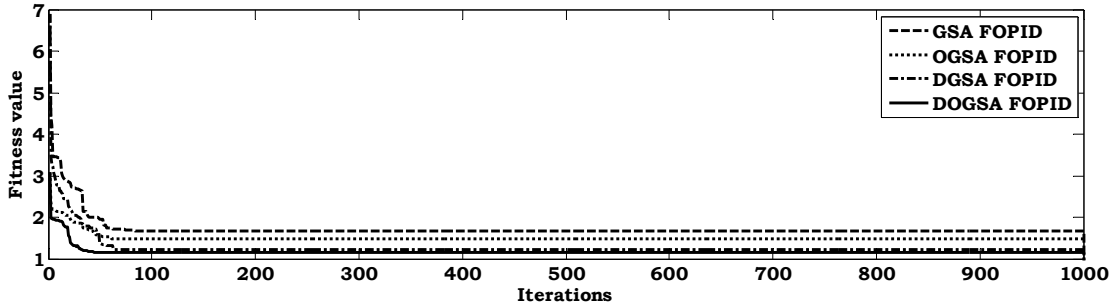

Figure 5. Comparative convergence profiles of GSA, OGSA, DGSA and DOGSA optimized FOPID controller

The eigen values of DOGSA optimized FOPID controlled system lies on left side of s-plane far away from origin as compared to its other variants which signifies more stability of the system. The least figure of demerit 0.00004339 is given by DOGSA which shows minimum steady state value and peak overshoot of deviations in frequency and tie-line power. The dynamic responses of area 1 are shown in Fig. 6 and Fig. 7.

C. Sensitivity Analysis

The robustness of the DOGSA tuned PID and FOPID controllers are also investigated against wide variations of system parameters. The operating load conditions, tie-line synchronizing coefficients, time constants of speed governor and turbine are varied in the range of +50% to -50% in steps of 25% taking at a time from their nominal values.

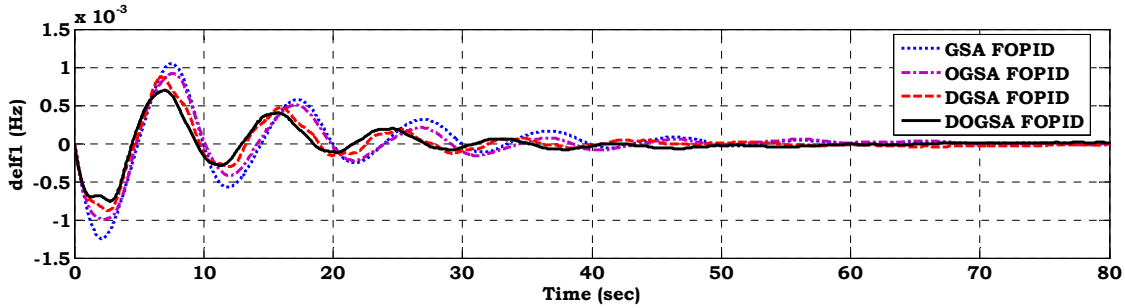

Figure 6. Frequency deviation in area 1 with optimized FOPID controller

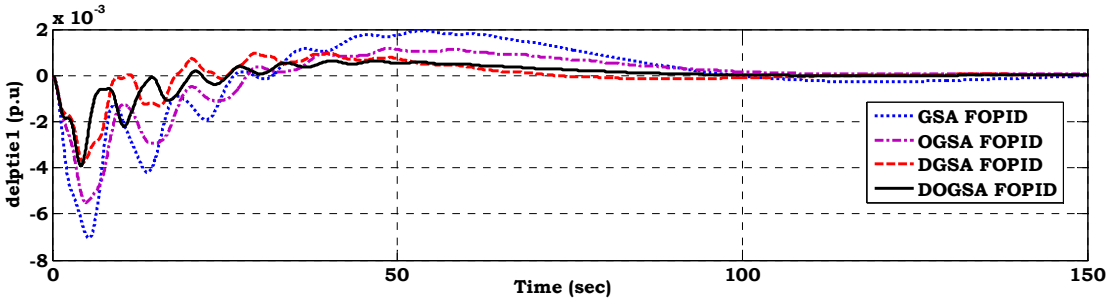

Figure 7. Tie-line power deviation in area 1 with optimized FOPID controller

TABLE III. COMPARISON OF EIGEN VALUES, DAMPING RATIO, SETTLING TIME, PEAK OVERSHOOT, FITNESS FUNCTION AND FIGURE OF DEMERIT VALUES FOR OPTIMAL FOPID CONTROLLED SYSTEM

Parameters	GSA	OGSA	DGSA	DOGSA
Eigen Values	-71.0995	-90.9355	-73.5529	-87.4911
	-64.9894	-72.1076	-70.4417	-70.5561
	-66.7984	-70.3182	-66.7114	-68.6652
	-69.4306	-71.3948	-65.6702	-65.6649
	-68.9816	-61.9441	-64.1718	-63.2453
	-68.1187	-64.2337	-62.7384	-61.8776
	-52.4727	-64.6581	-46.9606	-49.3325
	-44.2181	-50.5747	-42.5402	-48.8128
	-41.2667	-43.4044	-39.3610	-35.6396
	-30.4275	-39.6156	-37.6126	-36.7001
	-12.5396	-12.5790	-12.6267	-12.8588
	-12.5106	-12.5120	-12.5135	-12.5241
	-12.5000	-12.5000	-12.5000	-12.5000
	-4.7443	-0.1726 ± 2.1280i	-0.0499 ± 2.6459i	-0.0291 ± 3.5820i
	-4.5920	-4.6940	-4.8777	-4.9513
	-0.0353 ± 1.7383i	-4.5966	-4.4495 ± 0.1334i	-4.6478
	-3.9408	-4.2244	-3.9327	-4.5916 ± 0.1926i
	-0.0920 ±1.4084i	-4.2115	-0.3113 ± 1.5447i	-0.4119 ± 2.2978i
	-3.6261	-3.8664	-3.4397	-3.2738

	-3.2998 -3.1534 -3.2015 -3.1908 -0.0629 ± 0.6624i -2.4356 -1.4050 -1.3196 -0.9820 -1.8805 -2.0396 ± 0.0325i -2.0553 -2.0000 -2.5000 -0.2101 -0.0162 ± 0.1247i -0.0257 ± 0.1055i -0.0234 ± 0.0949i -0.0210 -0.0197 -0.0351 -0.0577 -0.1005 ±0.0200i -0.1163 -0.1506 -0.1449 -0.1471 -0.1460 -0.1410 -0.1000	-0.1542 ± 1.4184i -3.3596 -3.2636 -2.9972 -2.8752 -0.0848 ± 0.6590i -2.3475 -1.6999 -1.8414 -2.0252 -1.9723 -2.0000 -0.9085 -0.9212 -2.5000 -0.0311 ± 0.1277i -0.2162 -0.1949 -0.0294 ± 0.0524i -0.0217 ± 0.0303i -0.0200 -0.0290 -0.0362 -0.0433 -0.1017 ± 0.0189i -0.1538 -0.1345 -0.1478 -0.1391 -0.1399 -0.1000	-3.1604 -3.0963 -2.9187 -0.0813 ± 0.6953i -0.8256 -1.0056 ± 0.0744i -2.1877 -1.7472 -1.8287 -1.9646 -1.9745 -2.0000 -2.5000 -0.0340 ± 0.1607i -0.2473 -0.0126 ± 0.0820i -0.0098 ± 0.0513i -0.1024 ± 0.0642i -0.0301 -0.0225 -0.0235 -0.0827 -0.1583 -0.1479 -0.1425 -0.1329 -0.1247 -0.1181 -0.1000	-3.1215 -3.0691 -2.8725 -0.0788 ± 0.7119i -2.2917 -2.2812 -1.6570 -1.7035 -1.9442 -2.0000 -2.5000 -0.9031 -0.9262 -0.4733 -0.2382 -0.0181 ± 0.0964i -0.0719 ± 0.0925i -0.0319 ± 0.0822i -0.1737 -0.0334 ± 0.0539i -0.0186 -0.0281 -0.0273 -0.0911 -0.1325 -0.1418 -0.1398 -0.1359 -0.1016 -0.1000
Damping Ratio	0.0203	$2.10*10^{-5}$	0.0189	$6.57*10^{-7}$
Settling time (sec)				
Δf_1	53.99	49.27	47.29	46.61
Δf_2	70.05	69.11	68.43	63.41
Δf_3	63.45	55.46	52.70	50.85
ΔP_{tie1}	145.60	119.60	104.60	102.40
ΔP_{tie2}	156.30	132.10	112.80	112.70
ΔP_{tie3}	161.80	106.50	112.60	77.50
Peak overshoot				
Δf_1	0.001045	0.0009196	0.008673	0.000690
Δf_2	0.001267	0.0012400	0.001195	0.001165
Δf_3	0.001082	0.0009862	0.000978	0.000688
ΔP_{tie1}	0.003367	0.0014020	0.001324	0.001571
ΔP_{tie2}	0.008158	0.0067840	0.005074	0.006044
ΔP_{tie3}	0.003063	0.0022180	0.004917	0.001443
Steady state values				
Δf_1	0.0000185	-0.0000101	-0.0000129	0.000000199
Δf_2	0.00000973	0.00000506	-0.0000461	-0.0000269
Δf_3	0.0000353	0.0000429	-0.0000177	-0.0000140
ΔP_{tie1}	0.0000667	-0.0000616	-0.0000741	0.0000164
ΔP_{tie2}	0.000175	0.000123	0.0000429	-0.0000246
ΔP_{tie3}	-0.000121	-0.0000221	-0.000152	-0.0000831
Fitness value	1.6736	1.4742	1.2238	1.1522
FOD	0.00009118	0.00005631	0.00005482	0.00004339

a. Sensitivity Analysis of DOGSA Optimized PID Controller

The settling time and peak overshoot of the frequency and tie-line power deviations and damping ratio of the optimal PID controlled system are given in Table IV. It is observed that the overall system performance is hardly changed when the operating load condition and system parameters are varied. The frequency deviation responses of area 1 with different load conditions are shown in Fig. 8. which show that the DOGSA optimized PID controller gives robust and stable control to the system in case of wide variations in the nominal loading and other system parameters.

TABLE IV. SENSITIVITY ANALYSIS OF DOGSA TUNED PID CONTROLLER

Parameter Variation	**% change**	**Settling Time (sec)**						**Damping ratio**
		Δf_1	Δf_2	Δf_3	ΔP_{tie1}	ΔP_{tie2}	ΔP_{tie3}	
Loading condition	+25	55.84	60.1	58.85	107.7	180.1	180.9	0.0280
	-25	57.35	58.35	60.61	111.9	188.8	184.2	0.0280
	+50	65.4	60.11	64.89	109.6	187.2	185.6	0.0280
	-50	63.76	61.98	68.09	111.3	186.1	192.4	0.0280
T_g	+25	65.64	62.12	68.5	107.6	182.2	180.9	0.0296
	-25	63.53	61.64	62.96	108.2	185.6	187.9	0.0263

	+50	65.84	60.72	69.97	111.8	184.8	181.3	0.0283
	-50	69.92	60.21	61.73	109.8	187.5	173.5	0.0244
T_t	+25	67.35	65.58	67.61	117.6	271.8	378.3	0.0252
	-25	75.7	65.51	69.32	115.8	293.3	394.1	0.0219
	+50	78.89	61.88	68.95	119.3	275.8	403.7	0.0199
	-50	78.01	63.34	71.29	113.5	294.6	401.9	0.0138
T_{ij}	+25	42.83	52.9	57.38	187.4	130.2	142.1	0.0181
	-25	185.5	191.5	179.8	178.6	169.5	139.1	0.0086
	+50	70.45	68.17	58.7	169.7	87.28	142.3	0.0046
	-50	66.17	54.7	68.67	179.4	70.4	159.1	0.0054
Peak Overshoot								
Loading condition	+25	0.0004246	0.0006392	0.0004414	-0.00512	-0.010070	-0.006857	0.0280
	-25	0.0005906	0.0009132	0.0007680	-0.003345	-0.009928	-0.006478	0.0280
	+50	0.001027	0.001431	0.0012320	-0.01107	-0.019020	-0.013220	0.0280
	-50	0.000334	0.0003779	0.0003949	-0.004437	-0.005142	-0.004828	0.0280
T_g	+25	0.000588	0.001040	0.0006122	-0.004334	-0.01421	-0.008825	0.0296
	-25	0.0002029	0.000300	0.0002638	-0.003642	-0.008545	-0.007196	0.0263
	+50	0.0006974	0.0008207	0.0006411	-0.0082	-0.01494	-0.006635	0.0283
	-50	0.0002539	0.0004113	0.0002750	-0.003813	-0.009763	-0.005753	0.0244
T_t	+25	0.0004323	0.0006425	0.0005860	-0.004286	-0.01343	-0.012510	0.0252
	-25	0.0007153	0.0009800	0.0010450	-0.004331	-0.01453	-0.013690	0.0219
	+50	0.0007612	0.001078	0.0010760	-0.004428	-0.01402	-0.012070	0.0199
	-50	0.0005571	0.0009738	0.0006612	-0.004384	-0.01225	-0.008827	0.0138
T_{ij}	+25	0.0004857	0.0007136	0.0005422	-0.004591	-0.01307	-0.008720	0.0181
	-25	0.0007615	0.0012840	0.0007521	-0.004043	-0.01217	-0.008085	0.0086
	+50	0.0005427	0.0009845	0.0005458	-0.003534	-0.01669	-0.007275	0.0046
	-50	0.0006897	-0.0001836	0.0008677	-0.005182	-0.01333	-0.012760	0.0054

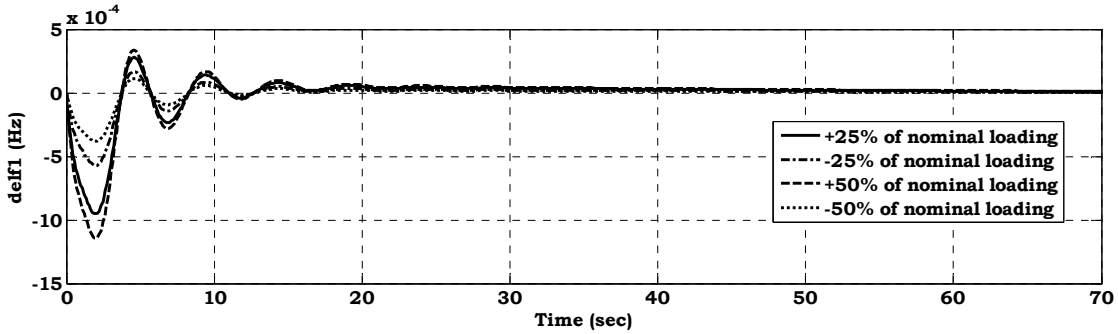

Figure 8. Frequency deviation of area 1 with DOGSA optimized PID controller for load disturbance of 0.1p.u MW with variation in loading

b. Sensitivity Analysis of DOGSA Optimized FOPID Controller

The damping ratio, settling time and peak overshoot of deviations in frequency and tie-line power for DOGSA optimized FOPID controller are given in Table V. From the simulation responses shown in Fig. 9 and system performance given in Table V, it has been concluded that the proposed control strategy provides a robust and stable control of the system and the controller parameters need not to be reset for wide changes in the system loading or parameters.

TABLE V. SENSITIVITY ANALYSIS OF DOGSA TUNED FOPID CONTROLLER

Parameter Variation	**% change**	**Settling Time (sec)**						**Damping ratio**
		Δf_1	Δf_2	Δf_3	ΔP_{tie1}	ΔP_{tie2}	ΔP_{tie3}	
Loading condition	+25	57.73	59.20	57.27	79.88	78.41	78.42	$6.57*10^{-7}$
	-25	51.76	54.35	52.03	78.40	77.54	79.41	$6.57*10^{-7}$
	+50	57.77	59.51	54.24	79.43	78.52	75.79	$6.57*10^{-7}$
	-50	50.64	54.38	50.18	79.16	78.14	79.04	$6.57*10^{-7}$
T_g	+25	78.95	57.56	56.42	77.08	78.45	78.80	$1.77*10^{-7}$
	-25	67.80	60.13	55.30	78.87	78.23	77.64	$2.12*10^{-8}$
	+50	51.01	58.94	59.34	76.20	77.43	77.16	0.0363
	-50	69.13	62.39	60.61	78.56	76.85	79.26	$9.07*10^{-7}$
T_t	+25	59.70	59.22	64.76	78.65	76.81	76.09	$4.16*10^{-8}$
	-25	58.95	60.31	65.73	77.50	78.98	77.53	$5.96*10^{-7}$
	+50	60.69	62.43	68.15	78.67	77.30	75.01	$6.57*10^{-7}$
	-50	60.09	60.40	60.13	78.93	74.19	76.73	0.1094
T_{ij}	+25	73.31	88.78	81.47	185.40	110.60	144.50	$2.17*10^{-7}$
	-25	71.94	99.59	96.70	188.50	99.80	142.60	$2.22*10^{-7}$
	+50	82.14	108.80	84.03	178.90	102.40	143.60	$3.06*10^{-7}$
	-50	150.60	167.60	169.30	175.40	177.20	166.20	$2.73*10^{-8}$
Peak Overshoot								
Loading	+25	0.0008831	0.0014560	0.0008597	0.001958	0.007523	0.001817	$6.57*10^{-7}$

condition								
	-25	0.0005296	0.0008714	0.0005150	0.001178	0.004544	0.001090	$6.57*10^{-7}$
	+50	0.0010600	0.0017480	0.0010330	0.002353	0.009085	0.002187	$6.57*10^{-7}$
	-50	0.0003522	0.0005824	0.0003443	0.000785	0.003026	0.000728	$6.57*10^{-7}$
T_g	+25	0.0010040	0.0011560	0.0007496	-0.00010	0.004834	-0.001831	$1.77*10^{-7}$
	-25	0.0011870	0.0007375	0.0007564	-0.00024	0.004222	-0.002003	$2.12*10^{-8}$
	+50	0.0003499	0.0006693	0.0006867	-0.00027	0.004843	-0.001549	0.0363
	-50	0.0012160	0.0007384	0.0007447	-0.00061	0.005129	-0.002011	$9.07*10^{-7}$
T_t	+25	0.0011720	0.0011720	0.0007126	0.001722	0.006058	0.002002	$4.16*10^{-8}$
	-25	0.0006865	0.0007068	0.0006768	0.001570	0.006050	0.001459	$5.96*10^{-7}$
	+50	0.0006851	0.0006865	0.0006342	0.001509	0.006044	0.001422	$6.57*10^{-7}$
	-50	0.0007059	0.0006709	0.0006813	0.001516	0.006025	0.001536	0.1094
T_{ij}	+25	0.0017840	0.0027850	0.0017220	0.001854	0.009176	0.001667	$2.17*10^{-7}$
	-25	0.0024700	0.0024400	0.0024100	0.002567	0.012220	0.002714	$2.22*10^{-7}$
	+50	0.0015960	0.0015960	0.0015300	0.001547	0.007925	0.001741	$3.06*10^{-7}$
	-50	0.0032060	0.0032060	0.003223	0.002631	0.014090	0.003991	$2.73*10^{-8}$

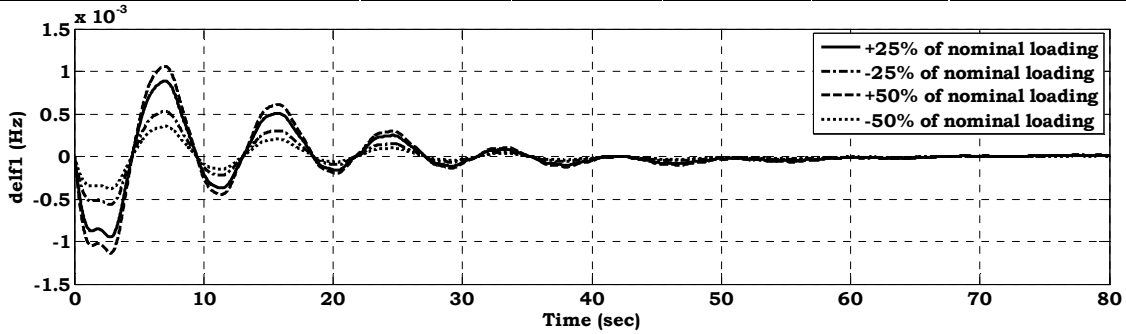

Figure 9. Frequency deviation of area 1 with DOGSA optimized FOPID controller for load disturbance of 0.1p.u MW with variation in loading

D. Handling of Physical Constraints

It is necessary to include the basic constraints imposed by the physical system dynamics and model them for the sake of performance evaluation to get an accurate discernment into the AGC problem. The generation rate constraint (GRC), time delay during signal processing in interconnected system and governor dead band are the important constraints which affects the power system. The values considered for these constraints are given in Table VI.

TABLE VI. PHYSICAL CONSTRAINTS

Parameter	Values
GRC	3% p.u MW
Governor deadband	0.036Hz
Time delay	2 sec

a. DOGSA Tuned PID Controller

The system dynamic responses of deviations in frequency and tie line power of area 1 including the physical constraints with optimized PID controller are shown in Fig. 10 and Fig. 11. The settling time and peak overshoot of deviations in frequency and tie-line power are given in Table VII. It is observed that the DOGSA optimized PID controller stabilizes the system even if the system becomes highly non-linear. The time delay and governor deadband cause a great overshoot/undershoot after a disturbance. But the controller successfully minimizes the frequency and tie-line power deviations to steady state in a considerable time.

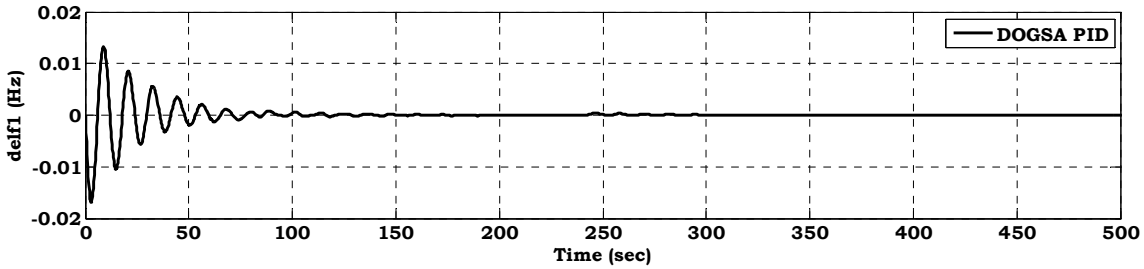

Figure 10. Frequency deviation of area 1 with optimized PID controller considering GRC, deadband and time delay

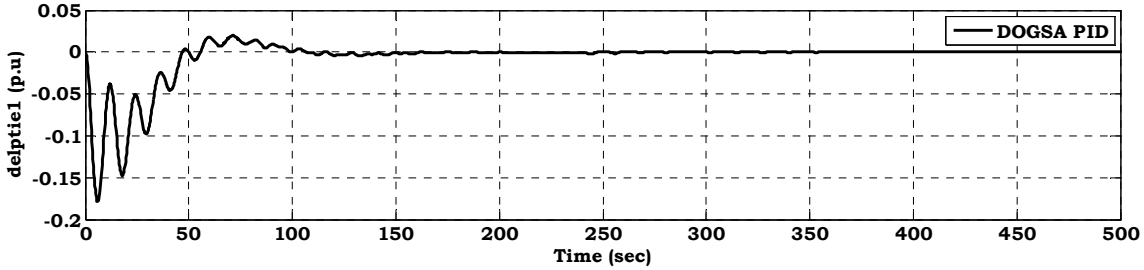

Figure 11. Tie-line power deviation of area 1 with optimized PID controller considering GRC, deadband and time delay

TABLE VII. SETTLING TIME AND PEAK OVERSHOOT OF PID CONTROLLED SYSTEM INCLUDING PHYSICAL CONSTRAINTS

Parameter	Settling time (sec)	Peak overshoot
Δf_1	357.50	0.01331
Δf_2	367.10	0.01335
Δf_3	369.80	0.01332
ΔP_{tie1}	329.40	-0.1787
ΔP_{tie2}	381.70	-0.1782
ΔP_{tie3}	492.90	-0.1785

b. DOGSA Tuned FOPID Controller

The simulation responses of DOGSA optimized FOPID controller including the physical constraints are shown in Fig. 12 and Fig. 13 for area 1. The settling time and overshoot of deviations in frequency and tie-line power given in Table VIII reveals that the proposed approach stabilizes the system rapidly as compared to PID controller.

TABLE VIII. SETTLING TIME AND PEAK OVERSHOOT OF FOPID CONTROLLED SYSTEM INCLUDING PHYSICAL CONSTRAINTS

Parameter	Settling time (sec)	Peak overshoot
Δf_1	57.83	0.009630
Δf_2	66.90	0.009326
Δf_3	75.19	0.009329
ΔP_{tie1}	142.50	0.012930
ΔP_{tie2}	153.30	-0.17770
ΔP_{tie3}	125.30	-0.17870

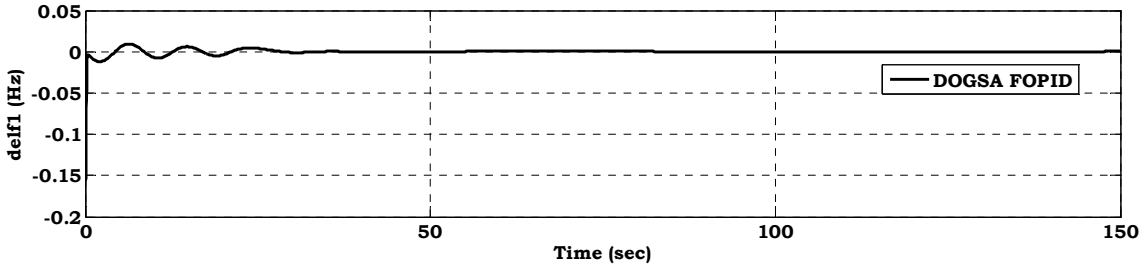

Figure 12. Frequency deviation of area 1 with optimized FOPID controller considering GRC, deadband and time delay

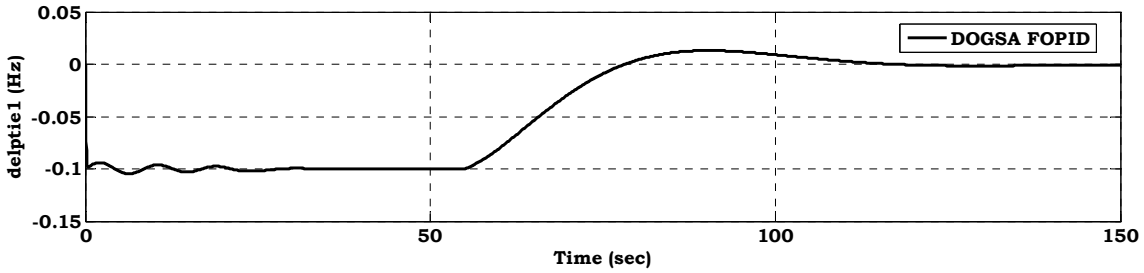

Figure 13. Tie-line power deviation of area 1 with optimized FOPID controller considering GRC, deadband and time delay

VI. CONCLUSION

The PID and FOPID controllers for AGC four area interconnected power system are tuned using GSA, OGSA, DGSA and DOGSA stochastic heuristic optimization techniques. The superiority of the hybridized DOGSA technique is investigated by comparing the convergence profile with other optimization techniques. The comparison of eigen values, damping ratio, settling time, peak overshoot and integral time absolute error shows the promising nature of proposed DOGSA technique. The optimized FOPID controller minimizes the frequency and tie line deviations faster as compared to tuned PID controller. The results obtained from the sensitivity analysis of the optimal PID and FOPID controlled system to wide variations in the system loading and parameters shows the robustness of the proposed controller. The proposed controller technique is also able to stabilize the power system effectively in the presence of non-linearities in the system.

APPENDIX A

Nominal values of parameters used in four area system models [25-27]

Parameter	Description	Value	Unit
f	Nominal frequency	60	Hz
P_{r1}, P_{r2}, P_{r3}	Rated generation of thermal, hydro and gas plant respectively	1000, 600, 250	MW
P_d	Nominal load	1000	MW
R_1,R_2,R_3,R_4,R_5	Regulations of governors in areas 1,2 and 3	2.4	Hz/p.u MW
B_1,B_2,B_3	Tie line frequency bias in areas 1, 2 and 3	0.425	p.u MW/Hz
T_{g1},T_{g2},T_{g3}	Governor time constants for thermal areas 1 and 3.	0.08	second
T_{t1},T_{t2},T_{t3}	Turbine time constants for thermal areas 1 and 3	0.4	second
K_{r1},K_{r2}	Reheater constraints (gains) for thermal reheat area 1	0.333	Thermal Unit
T_{r1},T_{r2}	Reheater time constants for thermal (reheat) area 1	10	second
K_{p1}, K_{p2}, K_{p3}	Power system gains of area 1, 2 and 3	120	Hz/p.u
T_{p1}, T_{p2}, T_{p3}	Power system load time constants of area 1, 2 and 3	20	second
T_1	Hydro governor (Stage 1) time constant for area 2	48.7	second
T_2	Hydro governor (Stage 2) time constant for area 2	0.513	second
T_3	Hydro governor (Stage 2) time constant for area 2	10	second
T_w	Water starting time for water turbine in area 2	1	second
T_{ij}	Synchronizing coefficients for tie lines between pair of areas for the four area system	0.0707	MW/radian
X	Gas governor lead time constant	0.6	second

Y	Gas governor lag time constant	1.0	second
a, c	Valve positioner constants	1	-
b	Valve positioner constant	0.5	-
T_{CR}	Combustion reaction time delay	0.3	second
T_F	Fuel time constant	0.23	second
T_{CD}	Compressor discharge volume time constant	0.2	second

APPENDIX B

Δf_k incremental frequency deviation in area k
ΔP_{tiek} net incremental real power exported from area k
$\Delta P_{int,\infty}$ net incremental real power exported from area considered to have infinite kinetic energy
ΔP_{tk} incremental real power generated from thermal reheat and non-reheat turbines
ΔP_{rk} incremental real power generated from reheat turbine
ΔP_{gk} change in steam valve position
ΔP_{tw} incremental real power generated from hydro turbine
ΔP_{Gk} change in hydro speed governor
ΔP_{TD} incremental real power generated from gas turbine
ΔP_{FC} incremental change in fuel combustor output
ΔP_{vp} change in gas valve positioner
ΔP_{sg} change in gas speed governor output

REFERENCES

[1] H. Saadat, Power system analysis, 2nd ed. New Delhi, India: TMH, pp. 551, 2002.

[2] Ibraheem, P. Kumar, D.P. Kothari, "Recent philosophies of automatic generation control strategies in power systems," IEEE T Power Syst, Vol. 20, No. 1, pp. 346–57, Feb. 2005. [Online]. http://dx.doi.org/10.1109/TPWRS.2004.840438

[3] H. Shayeghi, H.A. Shayanfar, A. Jalili, "Load frequency control strategies: A state-of-the-art survey for the researcher," Energ Convers Manage, Vol. 50, No. 2, pp. 344-353, Feb. 2009. [Online]. http://dx.doi.org/10.1016/j.enconman.2008.09.014

[4] S.K. Pandey, R.M. Soumya, N. Kishor, "A literature survey on load–frequency control for conventional and distribution generation power systems," Renew Sust Energ Rev, Vol. 25, pp. 318-334, Sep. 2013. [Online]. http://dx.doi.org/ 10.1016/j.rser.2013.04.029

[5] S.J.P.S. Mariano, J.A.N. Pombo, M.R.A. Calado, L.A.F.M. Ferreira, "A procedure to specify the weighting matrices for an optimal load-frequency controller," Turk J Electr Eng Co, Vol. 20, No. 3, pp. 367-379, 2012. [Online]. http://dx.doi.org/ 10.3906/elk-1003-413

[6] N. Hasan, Ibraheem, P. Kumar, N. Nizamuddin, "Sub-optimal automatic generation control of interconnected power system using constrained feedback control strategy," Int J Elec Power, Vol. 43, No. 1, pp. 295-303, Dec. 2012. [Online]. http://dx.doi.org/ 10.1016/j.ijepes.2012.04.039

[7] A. Demiroren, N.S. Sengor, H.L. Zeynelgil, "Automatic generation control by using ANN technique," Electr Pow Compo Sys, Vol. 29, No. 10, pp. 883–896, 2001. [Online]. http://dx.doi.org/10.1080/153250000152646505

[8] A. Zavoianu, G. Bramerdorfer, E. Lughofer, S. Siber, W. Amrhein, E.P. Klement, "Hybridization of multi-objective evolutionary algorithms and artificial neural networks for optimizing the performance of electrical drives," Eng Appl Artif Intel, Vol. 26, No. 8, pp. 1781-1794, Jun. 2013. [Online]. http://dx.doi.org/10.1016/j.engappai.2013.06.002

[9] E. Cam and I. Kocaarslan, "Load frequency control in two area power systems using fuzzy logic controller," Energ Convers Manage, Vol. 46, No. 2, pp. 233–243, Jan. 2005. [Online]. http://dx.doi.org/ 10.1016/j.enconman.2004.02.022

[10] M.I. Alomoush, "Load frequency control and automatic generation control using fractional order controllers," Electr Eng, Vol. 91, No. 7, pp. 357-368, Jan. 2010. [Online]. http://dx.doi.org/ 10.1007/s00202-009-0145-7

[11] H. Shayeghi, A. Jalili, H.A. Shayanfar, "Multi-stage fuzzy load frequency control using PSO," Energ Convers Manage, Vol. 49, No. 10, pp. 2570-2580, Oct. 2008. [Online]. http://dx.doi.org/ 10.1016/j.enconman.2008.05.015

[12] F. Valdez, P. Melin, O. Castillo, "An improved evolutionary method with fuzzy logic for combining particle swarm optimization and genetic algorithms," Appl Soft Comput, Vol. 11, No. 2, pp. 2625-2632, Mar. 2011. [Online]. http://dx.doi.org/10.1016/j.asoc.2010.10.010

[13] N. A. El-Hefnawy, "Solving bi-level problems using modified particle swarm optimization algorithm," Int J Artificial Intelligence, Vol. 12, No. 2, pp. 88-101, Oct. 2014.

[14] E.S. Ali, S.M. Abd-Elazim, "Bacteria foraging optimization algorithm based load frequency control for interconnected power system," Int J Elec Power, Vol. 33, No. 3, pp. 633-638, Mar. 2011. [Online]. http://dx.doi.org/ 10.1016/j.ijepes.2010.12.022

[15] U.K. Rout, R.K. Sahu, S. Panda, "Design and analysis of differential evolution algorithm based automatic generation control for interconnected power system," Ain Shams Eng J, Vol. 4, No. 3, pp. 409-421, Sep. 2013. [Online]. http://dx.doi.org/ 10.1016/j.asej.2012.10.010

[16] H. Shabani, B. Vahidi, M. Ebrahimpour, "A robust PID controller based on imperialist competitive algorithm for load-frequency control of power systems," ISA T, Vol. 52, No. 1, pp. 88-95, Jan. 2013. [Online]. http://dx.doi.org/10.1016/j.isatra.2012.09.008

[17] S. Debbarma, L.C. Saikia, N. Sinha, "Automatic generation control using two degree of freedom fractional order PID controller," Int J Elec Power, Vol. 58, pp. 120-129, Jun. 2014. [Online]. http://dx.doi.org/10.1016/j.ijepes.2014.01.011

[18] E. Rashedi, H. Nezamabadi-pour, J.S. Saryazdi, "GSA: a gravitational search algorithm," Inform Sciences, Vol. 179, No. 13, pp. 2232–2248, Jun. 2009. [Online]. http://dx.doi.org/ 10.1016/j.ins.2009.03.004

[19] R.K. Sahu, S. Panda, S. Padhan, "Optimal gravitational search algorithm for automatic generation control of interconnected power systems," Ain Shams Eng J, Vol. 5, No. 3, pp. 721-733, Sep. 2014. [Online]. http://dx.doi.org/10.1016/j.asej.2014.02.004

[20] R. E. Precup, R. C. David, E. M. Petriu, S. Preitl, A. S. Paul, "Gravitational search algorithm-based tuning of fuzzy control systems with a reduced parametric sensitivity," Series: Soft Computing in Industrial Applications, Advances in Intelligent and Soft Computing, Vol. 96, pp. 141-150, 2011. [Online]. http://dx.doi.org/10.1007/978-3-642-20505-7_12

[21] S. Rahnamayan, H.R. Tizhoosh, M.M.A. Salama, "A novel population initialization method for accelerating evolutionary algorithms," Comput Math Appl, Vol. 53, No. 10, pp. 1605-1614, May 2007. [Online]. http://dx.doi.org/ 10.1016/j.camwa.2006.07.013

[22] B. Shaw, V. Mukherjee, S.P. Ghoshal, "A novel opposition-based gravitational search algorithm for combined economic and emission dispatch problems of power systems," Int J Elec Power, Vol. 35, No. 1, pp. 21-33, Feb. 2012. [Online]. http://dx.doi.org/10.1016/j.ijepes.2011.08.012

[23] S. Sarafrazi, H. Nezamabadipour, S. Saryazdi, "Disruption: a new operator in gravitational search algorithm," Sci Iran, Vol. 18, No. 3, pp. 539-548, Jun. 2011. [Online]. http://dx.doi.org/ 10.1016/j.scient.2011.04.003

[24] A.W. Berger, F.C. Schweppe, "Real time pricing to assist in load frequency control," IEEE T Power Syst, Vol. 4, No. 3, pp. 920-926, Aug. 1989. [Online]. http://dx.doi.org/ 10.1109/59.32580

[25] I.C. Report, "Dynamic model for steam and hydro turbines in power system studies," IEEE T Power Ap Syst, Vol. PAS-92, No. 6, pp. 1904-1915, Nov. 1973. [Online]. http://dx.doi.org/10.1109/TPAS.1973.293570

[26] I.W.G. Report, "Dynamic models for fossil fuelled steam units in power system studies," IEEE T Power Syst, Vol. 6, No. 2, pp. 753-761, May 1991. [Online]. http://dx.doi.org/ 10.1109/59.76722

[27] W.I. Rowen, "Simplified mathematical representation of heavy duty gas turbine," J Eng Gas Turb Power, Vol. 105, No. 4, pp. 865-870, Oct. 1983. [Online]. http://dx.doi.org/ 10.1115/1.3227494